1 # Subsurface manifestation of Marine Heatwaves in the South West

2 # Indian Ocean

3 Clea B. Welch[1,2], Neil Malan[3], Daneeja Mawren[1,2],Tamaryn Morris[2], Janet Sprintall[4],Juliet C. Hermes[1,2]

4 [1]Ocean and Atmosphere Science, University of Cape Town, Cape Town, 7700, South Africa
5 [2]South African Environmental Observation Network Egagasini node, Cape Town, South Africa
6 [3]Climate Change Research Centre and Centre of Marine Science and Innovation, University of New South Wales, Sydney,
7 New South Wales, Australia
8 [4]Scripps Institution of Oceanography, University of California, San Diego, La Jolla, CA, United States

9 *Correspondence to*: Clea B. Welch (wlccle001@myuct.ac.za)

10 **Abstract.** Marine heatwaves (MHW) are extreme events of prolonged, anomalously warm ocean temperatures. Globally,
11 marine heatwaves are increasing in frequency and intensity and are responsible for long-term impacts on marine ecosystems,
12 which have devastating socio-economic consequences. A key gap in our understanding of MHWs is how they manifest in the
13 subsurface. This paper uses satellite sea surface temperature (SST) data and *in situ* subsurface temperature observations from
14 Expendable Bathythermographs (XBTs) to investigate the anomalous water temperature characteristics associated with surface
15 identified MHWs in the South West Indian Ocean (SWIO) and how they progress through the water column. We find that the
16 eddy corridors through the SWIO, where EKE is high and SST variability is low, are primarily characterised by the occurrence
17 of abrupt and intense MHWs, and that the frequency, duration and intensity of these events are largely associated with
18 mesoscale activity. In these eddy corridors, surface–detected MHW case studies demonstrate a strong, deep–reaching
19 subsurface temperature anomaly signal with maximum intensity below the surface. The majority of these MHWs are associated
20 with anticyclonic eddies, which provide a possible mechanism for the deep extent of the surface MHWs. Improving our
21 understanding of the interaction between mesoscale features and subsurface MHW characteristics will benefit prediction of
22 MHWs and management of the regions' biodiversity.~~that the SWIO, which is dominated by the presence of mostly warm
23 anticyclonic eddies, is characterised by moderate MHWs, and that the frequency, duration and intensity of these events are
24 largely associated with mesoscale activity. Surface–detected MHW case studies demonstrated a strong subsurface temperature
25 anomaly signal, with maximum intensity below the mixed layer depth. The spatial distribution of anticyclonic, warm–core
26 eddies closely matched the distribution of the MHWs. This provides a possible mechanism for the deep extent of these surface
27 MHWs. Improving our understanding of the interaction between mesoscale features and subsurface MHW characteristics will
28 benefit prediction of MHWs and management of the regions' biodiversity.~~

1 Introduction

Marine heatwaves (MHWs) are extreme, anomalously warm ocean events that are known to have devastating impacts on marine species, ecosystems, and ultimately coastal countries' socioeconomics that depend on a blue economy (Mills et al., 2013; Hobday and Pecl, 2014; Hermes et al., 2019). The thermal stress during MHWs has initiated coral bleaching events, destroyed marine foundation species, caused mass mortality events, species redistributions and resulted in irreversible physiological damage to marine life (Mills et al., 2013; Frölicher et al., 2018; Oliver et al., 2021; Perez et al., 2021; Garrabou et al., 2022; Mawren, et al., 2022 b). The adverse effects of MHWs are especially concerning as, under scenarios of continued global ocean warming, MHWs are projected to increase globally, with events lasting longer and intensifying. If this trend continues many parts of the ocean are predicted to reach a near-permanent MHW state by the late 21st century (Hobday et al., 2016; Frölicher et al., 2018; Oliver et al., 2018; Holbrook et al., 2020). This highlights the need for rapid improvement in our understanding of MHWs and how to manage or adapt to their impacts (Elzahaby and Schaeffer, 2019).

A key gap in our understanding of MHW events is how they manifest in the subsurface (Oliver et al., 2018). MHW detection and characterization is largely limited to the surface due to the lack of continuous, long-term, and high-resolution subsurface temperature records (Elzahaby et al., 2021). However, MHWs themselves are not surface trapped, as they can penetrate to considerable depths, or even exist at depth with no surface signal (Elzahaby and Schaeffer, 2019; Holbrook et al., 2020; Scannell et al., 2020; Elzahaby et al., 2021; Schaeffer, Sen Gupta and Roughan, 2023; Zhang et al., 2023). The lack of subsurface MHW characterisation limits our understanding of the true impacts these events have, as it is the vertical extent of MHWs that directly impact marine ecosystems (Elzahaby and Schaeffer, 2019; Holbrook et al., 2020; Scannell et al., 2020).

The subsurface extent of MHWs is often associated with different spatial MHW patterns and drivers compared to the surface (Elzahaby and Schaeffer, 2019; Scannell et al., 2020; Perez et al., 2021; Fragkopoulou et al., 2023; Zhang et al., 2023). Different ocean dynamical processes, such as large-scale circulation, oceanic planetary waves, boundary currents, eddies, local downwelling, seasonal stratification and mixing influences the vertical structure of MHWs (Schaeffer, Sen Gupta and Roughan, 2023; Zhang et al., 2023). Upper ocean MHWs (0-150 m) have been shown to mostly originate from anomalous air-sea fluxes, but even in cases where air-sea heat fluxes are the predominant driver of MHWs, ocean dynamical processes can extend the warm MHW signature into the subsurface (Schaeffer, Sen Gupta and Roughan, 2023; Zhang et al., 2023). Deeper MHWs (that extend below 150m) are shown to be mostly driven by deep warm-core, anticyclonic mesoscale eddies (Schaeffer and Roughan, 2017; Elzahaby and Schaeffer, 2019; Perez et al., 2021; Fragkopoulou et al., 2023), boundary current shifts (Großelindemann et al., 2022) and Ekman pumping (Hu et al., 2021). In particular, eddies in subtropical western boundary currents (WBCs) are known to drive deeper and longer-lasting MHWs (Schaeffer and Roughan, 2017; Elzahaby and Schaeffer, 2019; Benthuysen et al., 2020; Elzahaby et al., 2021; Zhang et al., 2023).

Here, the focus is on the South West Indian Ocean (SWIO), which is part of the greater western Indian Ocean global warming hotspot (Roxy et al., 2014), and is host to a highly unique, complex and variable WBC current system that supports one of the six primary global marine biodiversity hotspots (Ramirez et al., 2017). This makes assessing MHWs in this region even more

62   crucial and urgent, yet to date, MHW characterization in this region is sparse and limited to the surface (Mawren et al., 2022

63   a).

64

(a) South West Indian Ocean dynamics
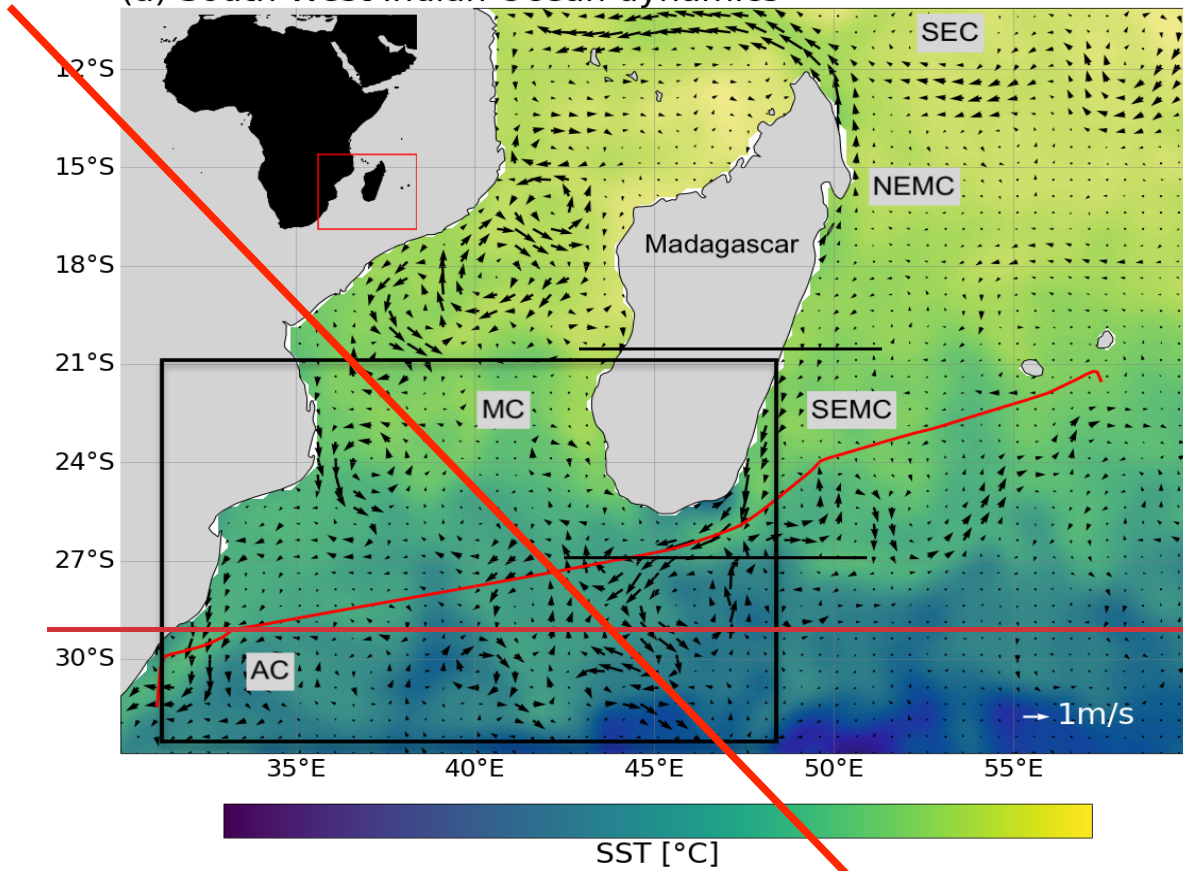
(b) Number of XBT Transects

65
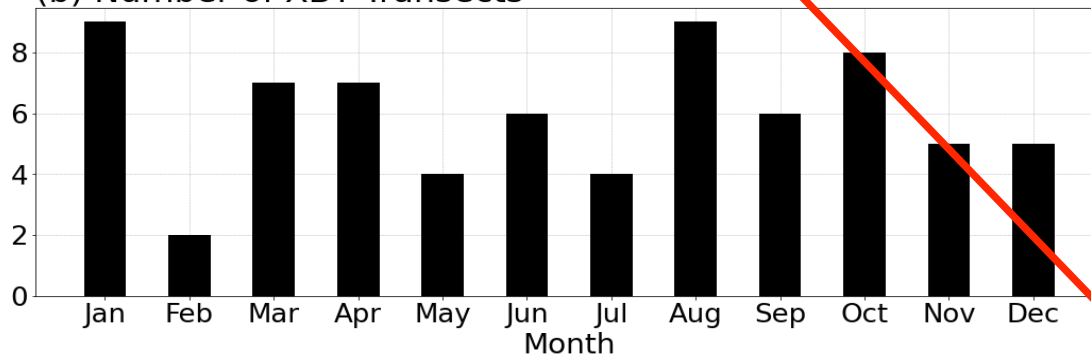
Figure 1: (a) A snapshot of sea surface temperature conditions on 13/04/2021 (OISST V2) of the South West Indian Ocean, with geostrophic current velocities overlaid (satellite AVISO altimeter). Key ocean circulation features are highlighted - SEMC South-East Madagascar Current, NEMC North-East Madagascar Current, SEC South Equatorial Current, Mozambique Channel and Agulhas Current. The black box 22° S - 32° S and 31° E - 48° E) indicates the study area. The red line represents the IX21 HR-XBT transect from Durban, South Africa to Port Louis, Mauritius. **(b)** The number of XBT transects available for each month from the IX21 transect for the period from 1994 – 2022.

 A key feature in the SWIO is the Greater Agulhas Current System which consists of the eddying flow through the Mozambique Channel (MC) and two dynamic WBCs, the South East Madagascar Current (SEMC) and the Agulhas Current (AC), the largest and strongest Southern Hemisphere WBC, which plays a vital role in global thermohaline circulation (Fig. 1; Beal et al., 2020). Flow through the MC is characterised by large, deep-reaching, mostly anticyclonic and anomalously warm southward propagating mesoscale eddies, which are formed from baroclinic instability in the South Equatorial Current (SEC), around the Comoros Islands (Collins et al., 2012; Halo et al., 2014; Voldsund et al., 2017). South of Madagascar, the SEMC retroflects and sheds pairs of counter-rotating mesoscale eddies which converge with eddies from the MC (Voldsund et al., 2017). The persistence of eddies from the MC and SEMC creates a state of instability, which is the main source of variability and SST anomalies in the region, making this region especially susceptible to the occurrence of MHWs (DiMarco et al., 2000; Halo et al., 2014; Phillips et al., 2021; Mawren et al., 2022 a).

Where the MC and SEMC converge, eddy activity is highest, and surface-identified MHWs are increasing in frequency, intensity and duration more rapidly than anywhere else in the MC (Mawren et al., 2022 a). Intensification of mesoscale eddies, has subsequently increased ocean warming trends and SST anomalies, which may largely explain these observed MHW trends (Wu et al., 2012; Schaeffer and Roughan, 2017; Benthuysen et al., 2020; Mawren et al., 2022 a). The most intense and longest-lasting MHW in the MC occurred in February 2017 (Mawren et al., 2022 a). The 2017 MHW event was found to be modulated by horizontal advection and the presence of mesoscale eddies, with maximum temperature anomalies peaking when the core of an anticyclonic eddy passed through (Mawren, Hermes and Reason, 2022 a). This suggests that, as seen in other WBC regions (Bian et al., 2023), mesoscale eddies significantly influence the occurrence and intensity of MHWs in the SWIO (Mawren et al., 2022 a). Yet, the exact role mesoscale eddies play in driving surface MHW characteristics and their subsurface extent, remains unclear. This is of particular concern as the SWIO supports a variety of temperature-sensitive, pristine ecosystems with high biological diversity, high endemism and endangered species. The disruption to the ecosystem can have significant socioeconomic impacts, as neighbouring east African countries rely heavily on these ecosystems for fish stocks and marine ecotourism (Obura, 2012; Pereira et al., 2014).

This study aims to build on the limited work that has previously explored MHW events and trends in the SWIO with a focus on their subsurface characteristics. In Section 2, data sets and methodology are described. Section 3 investigates surface MHW characteristics, then, using temperature profiles from in situ Expendable Bathythermographs (XBTs) observations, the subsurface extent of surface-identified MHWs are explored. This provides the first description of subsurface characteristics of MHWs in the SWIO. Particular focus is also placed on understanding the role mesoscale eddies play on both the surface and subsurface extent of MHWs. For this reason, the study area is confined to 22° S - 32° S and 31° E - 48° E, which encompasses the region of greatest ocean variability and mesoscale eddy activity south and southwest of Madagascar (Fig. 1). A Discussion follows in Section 4 with Conclusions in Section 5.

2 Methods

2.1 Sea surface temperature and surface marine heatwave identification

High resolution gridded (0.25°) NOAA optimally interpolated sea surface temperature (OI SST) V2 data was used to explore SST conditions and identify surface MHWs in the SWIO region from 01/01/1993 – 31/12/2022~~1993 – 2022~~. This time period matches the same time period of available XBT data, used to investigate the subsurface extent of surface–identified MHWs. OISST data has been widely used to identify and characterise global and regional MHW events and trends globally (Reynolds et al., 2007; Banzon et al., 2016; Frölicher et al., 2018; Sen Gupta et al., 2020; Guo et al., 2022; Saranya et al., 2022) and in the SWIO (Mawren et al., 2022 a; Mawren et al., 2022 b).

MHWs were identified and quantified in the SWIO using the Hobday et al., (2016) definition, which defines a MHW as a discrete, anomalously warm water event, with temperatures that exceed the 90th percentile (the threshold) of the 30-year historical baseline period and have a duration of at least five consecutive days. For consistency with previous studies, a fixed climatological baseline, 1993–2022, and a 31 day smoothing window was used to identify surface MHWs (Smith et al., 2025)~~A fixed climatological baseline and a 31 day smoothing window was used to identify surface MHWs~~. The properties of MHWs over the region were described by set metrics: mean duration (the time, in days, between the start and end of a MHW), mean frequency (the number of events that occurred during a year or season), mean intensity (the average temperature anomaly over the duration of the event) and the cumulative intensity (integrated temperature anomaly for the duration of the event). Seasonal MHW patterns were also investigated using the metric cumulative intensity, which provides a good description of the severity of MHW events (Mawren et al., 2021). Detected MHW events over the entire climatological mean were grouped by austral season (Summer–December, January and February; Autumn–March, April and May; Winter–June, July and August and Spring–September, October and November).

2.2 Subsurface temperature measurements from *in situ* data

The subsurface expression of surface MHWs (detected from OISST data) was investigated using XBT data from the near-repeat IX21 HR-XBT transect. XBTs provide temperature profiles from 0 to 850 m depth. IX21 is nominally from Durban, South Africa (29.9° S, 31.0° E) to Port Louis, Mauritius (20.2° S, 57.5° E) (Chandler et al., 2022), but for this study, the portion of the IX21 transect from Durban to south of Madagascar was used.

The IX21 HR-XBT transect is nominally occupied 4 times a year and has a horizontal resolution of 6 – 10 km between XBT profiles within the boundary current and 20–30 km offshore (Goni et al., 2019; Chandler et al., 2022). The transect takes three days to complete and so is considered synoptic. Each transect is assigned the date of the first temperature profile acquired for the cruise. Temperature was objectively mapped to 10m depth intervals from 0m to 800 m and 0.1° intervals in longitude (Chandler et al., 2022). Data was available from 8 September 1994 to 6 September 2022. Since XBT data from the IX21 transect is collected nominally 4 times a year, there is not enough data to produce a high-resolution climatological baseline period, which is required to identify MHWs using the Hobday et al., (2016) definition.

138 Instead, subsurface temperature anomalies calculated relative to the seasonal climatological means, calculated using the XBT
139 data (Fig. 1b), from 1994 – 2022 were used as the measure of the subsurface extent of surface MHWs, an approach commonly
140 used when studying subsurface MHW signals using in situ data (Schaeffer and Roughan, 2017; Elzahaby and Schaeffer, 2019;
141 Elzahaby et al., 2021; Perez et al., 2021). Each seasonal mean consisted of ~15–20 XBT transects (Fig. 1b). To calculate
142 temperature anomalies, the seasonal climatological means were subtracted from the daily temperature profiles for each data
143 available day.

144 **2.3 Sea level anomaly data**

145 To investigate the influence of mesoscale eddies on the properties of surface-identified MHWs, high resolution (0.25°),
146 optimally integrated, gridded daily sea level anomalies (SLA) and geostrophic currents, over a thirty–year period (01/01/1993
147 – 31/12/2022) sea level anomalies (SLA) and geostrophic currents, over a twenty–year period (1993 – 2012), were extracted
148 from altimeter satellite data distributed by AVISO (Archiving, Validation, and Interpretation of Satellite Oceanographic data).
149 Altimeter satellite gridded SLA are computed with respect to a twenty–year [1993, 2012] mean. This data has previously been
150 used to track eddies during MHWs in the SWIO by Mawren et al. (2022a). In the SWIO, where in situ observations are sparse,
151 satellite altimetry provides useful information about mesoscale ocean variability and is the best way to identify the presence
152 of mesoscale eddies (Halo et al., 2014). Positive (negative) SLA associated with anticyclonic (cyclonic) geostrophic currents
153 indicate the presence of warm-core (cold-core) eddies (Halo et al., 2014).
154 Mean eddy kinetic energy (EKE) for the entire time period was calculated using SLA and geostrophic velocity and used as a
155 measure of eddy activity across the region. Mean EKE was calculated as:

156 $$\text{EKE} = \frac{1}{2}(u'^2 + v'^2), \tag{1}$$

157 where u'^2 represents the mean squared anomaly of the horizontal velocity component u from its spatial mean and v'^2 represents
158 the mean squared anomaly of the vertical velocity component v from its spatial mean (Bai et al., 2024).

159 **2.4 Investigation of subsurface anomaly signals associated with surface MHWs**

160 For each day when subsurface data from the IX21 XBT transect were available, and a MHW signal was detected at the
161 corresponding location, the associated subsurface warm temperature signal was isolated. These subsurface warm temperature
162 anomaly profiles were used to investigate the subsurface manifestation of surface identified MHWs. The corresponding surface
163 SLA for each anomaly profile was also recorded to further investigate the influence of mesoscale eddies on the characteristics
164 of the subsurface anomaly. By correlating the SLA with the temperature anomaly profiles, the analysis aimed to uncover
165 potential links between mesoscale ocean dynamics and the vertical extent, intensity, and structure of subsurface temperature
166 anomalies associated with surface MHWs. This dual focus on both subsurface and surface parameters provides a
167 comprehensive framework for investigating the complex interactions driving the subsurface expression of marine heatwaves.

3 Results

3.1 Surface MHW variability

The SWIO is defined by distinct spatial patterns that characterize MHW related variability (Fig. 2c–f) that are underpinned by pre–existing mean SST conditions and variability (Fig. 2). ~~The SWIO is defined by distinct spatial patterns of mean annual surface MHW characteristics that are underpinned by pre-existing mean SST conditions and variability (Fig. 2).~~ On the other hand, despite distinct seasonality in mean SST and variability, MHWs do not exhibit strong seasonality, as the spatial pattern of MHW cumulative intensity remains similar during each season (Not shown). Due to the lack of observed MHW seasonality, the mean MHW trends and their relationship with SST variability and mesoscale eddies are further investigated.

The SWIO experiences warm mean ocean temperatures, up to 28 ℃ , in the Mozambique Channel (21° S) that decrease southward, reaching a minimum of 19 ℃ at 33° S (Fig. 2a). The SST standard deviation shows that, on average, the majority of the region experiences SSTs that exceed the mean by between 1.5–2.2 ℃ (Fig. 2b). On average, surface MHWs occur 1 to 3 times per year, last 8–18 days and reach intensities of 1.0–2.0 °C, but have varying spatial characteristics (Fig. 2b – f). These observed mean values of MHW frequency, duration, intensity and cumulative intensity, are consistent with previous findings by Mawren et al. (2021) in the SWIO, and global WBC studies by Oliver et al. (2018) and Holbrook et al. (2019). Within the southern MC, MHWs occur most frequently (between 2–3 times on average per year), but are shorter-lived (8–12 days) and less intense (1.2–1.5 ℃), whereas, in the southeast open ocean region, MHWs occur less frequently (between 1–2 times on average per year), but are longer-lasting (12–18 days) and more intense (1.4–2.2 ℃) (Fig. 2c,d). Similarly, since cumulative intensity is the integration of duration and intensity, MHWs are the most severe (16–19 ℃days) in the southeast open ocean, and least severe in the southern MC (8–16 ℃days) (Fig. 2f).

189
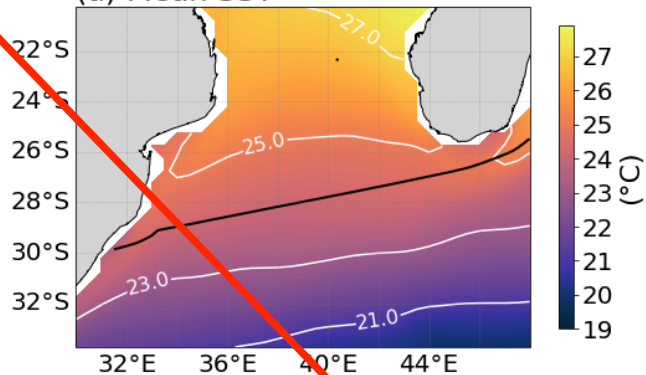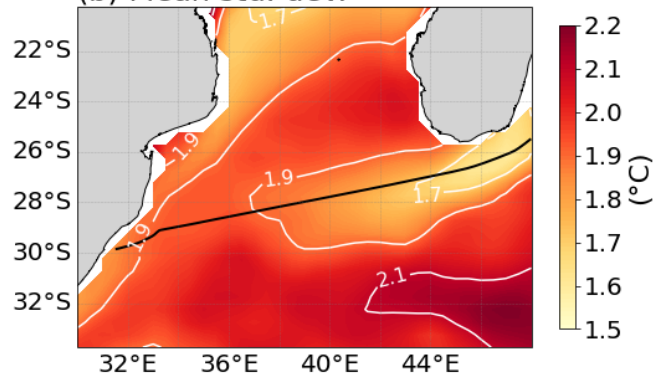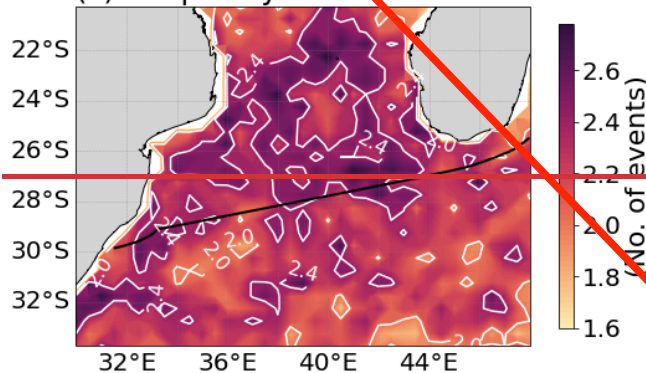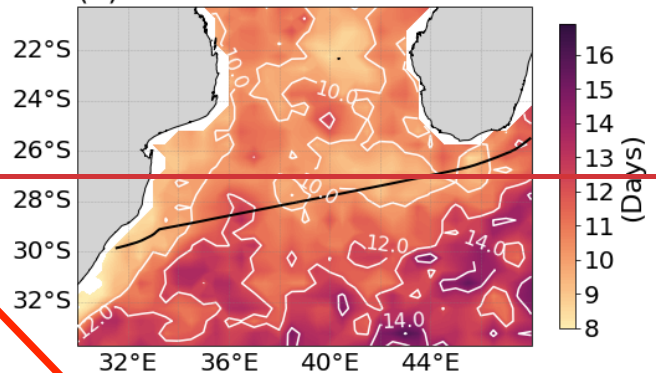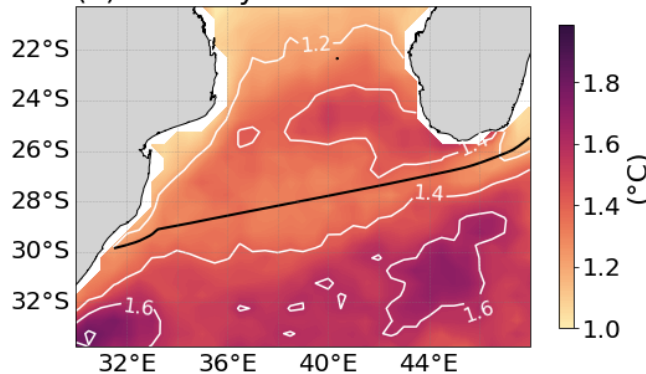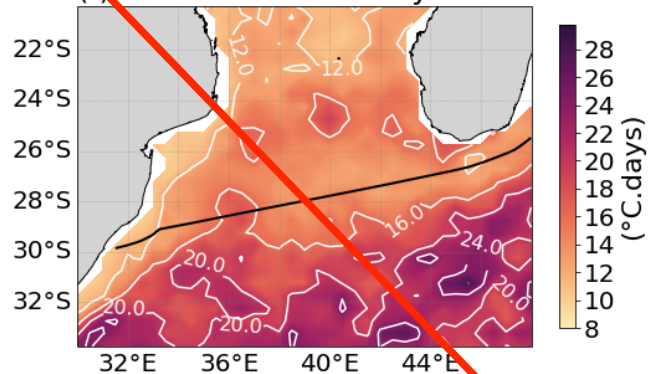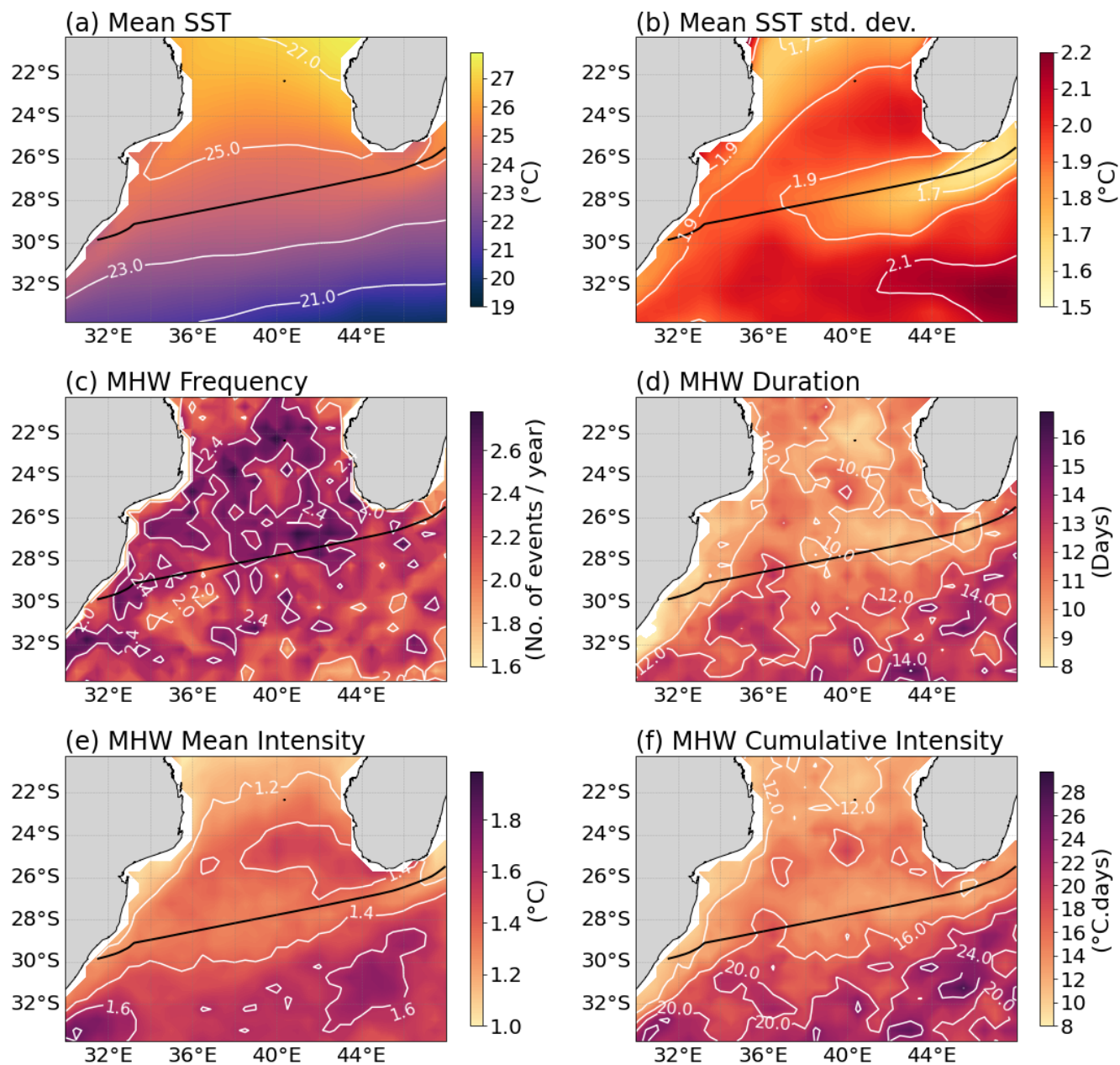
Figure 2: Climatological mean **(a)** SST (℃) and **(b)** SST standard deviation (℃). Surface mean annual MHW **(c)** frequency, **(d)** duration (days), **(e)** mean intensity (℃) and **(f)** cumulative intensity (℃Cdays) calculated from NOAA optimally interpolated sea surface temperature (OISST V2) high resolution (0.25°) gridded SST data for the climatological period from 1993–2023. The black solid line in all the figures denotes the IX21 XBT transect.

The mean annual spatial distribution of MHW characteristics is closely linked to the underlying patterns of SST variability. Regions with higher SST variability are associated with more intense MHW intensity, as evidenced by a strong correlation (r = 0.75, p–value > 0.05) (Fig. 3b). SST variance is highest off the west coast of Madagascar (1.5 °C) and in the southern–most open ocean (1.9–2.2 °C) but is weakest along the west coast of Africa and at the region of SEMC leakage (Fig. 3b), confirming the spatial relationship between SST variance and MHW intensity (Fig. 2e, Fig. 3b). ~~The mean spatial distribution of MHW characteristics are largely related to the underlying patterns of SST variability (Fig. 2). As is seen in the mean spatial distribution of MHW intensity, SST variance is highest off the west coast of Madagascar (1.5 °C) and in the southern–most open ocean (1.9–2.2 °C) but is weakest along the west coast of Africa and at the region of SEMC leakage (Fig. 2b), implying MHW intensity is closely associated with SST variance (Fig. 2b and e).~~ Weaker SST variance within the southern MC and along the west coast of Africa, compared to the southernmost open ocean region, also closely resembles the patterns of MHW duration and cumulative intensity, which suggests that longer (shorter)-lasting and more (less) severe MHWs are associated with higher (lower) SST variance (Fig. 2b, d, f). Unlike MHW duration, intensity and cumulative intensity, the mean spatial distribution of MHW frequency reflects an inverse pattern compared to SST variance, suggesting that where SST variance is high (low), MHWs occur less (more) often (Fig. 2b, c).

To investigate the role that underlying oceanographic processes play in driving the observed mean surface MHW characteristics, we investigate the relationship between EKE, geostrophic velocities and SST variability (Fig. 3a). The westward–flowing SEMC leakage is visible, as is the train of eddies flowing southward through the MC and the fast, southward–flowing AC (Fig. 1a and 3a). EKE is strongest on the western side of the MC and between the southern tip of Madagascar and the continent, where stronger poleward and south–westerly currents are present, respectively (Fig. 3b). Furthermore, the significant correlation between SST variability and MHW intensity is closely linked to EKE (Fig. 3b). Regions with high EKE (0.08–0.16 m²/s²) exhibit low SST variability and are characterized by frequent, short–lived, and less intense MHWs. This suggests that high EKE, driven by the mean surface flow, promotes the formation of MHWs but also accelerates their dissipation due to shorter residence times. Conversely, regions with low EKE (0.0–0.08 m²/s²) experience higher SST variability and support less frequent but more intense and longer–lasting MHWs. This implies that reduced EKE allows for more stable thermal conditions, fostering the persistence of intense MHW events (Fig. 2b, c; Fig. 3). This observed relationship reinforces the role of local thermal fluctuations in driving extreme ocean warming. ~~To investigate the role that underlying oceanographic processes play in driving the observed mean surface MHW characteristics, mean EKE and geostrophic velocities are shown, with SST variability overlain as contours (Fig. 3). The westward flowing SEMC leakage is visible, as is the train of eddies flowing southward through the MC and the fast, southward flowing AC (Fig. 1a and 3). EKE is strongest on the western side of the MC and between the southern tip of Madagascar and the continent, where stronger poleward and south westerly currents are present (respectively) (Fig. 3).~~

~~There is a clear relationship between the spatial patterns of the mean surface MHW metrics and EKE (Fig. 2 and 3). Regions with high EKE (0.08–0.16 m²/s²) align with the regions where, on average, SST variability is relatively low and MHWs occur~~

233 ~~more frequently, but are relatively shorter-lived and less intense, suggesting that the presence of energetic eddies increases the~~
234 ~~occurrence and then dissipation of MHW events (Fig. 2b and c and Fig. 3). The regular propagation of eddies with mean~~
235 ~~surface flow through these regions results in eddies with short residence times consistently passing through the region, causing~~
236 ~~frequent MHWs with short lifespans. On the other hand, where EKE is low (0.0 - 0.08 m²/s²) corresponds to regions where~~
237 ~~observed mean SST variability is relatively high and annual mean MHWs occur less frequently but are longer-lasting and more~~
238 ~~intense (Fig. 2b and c and Fig. 3).~~
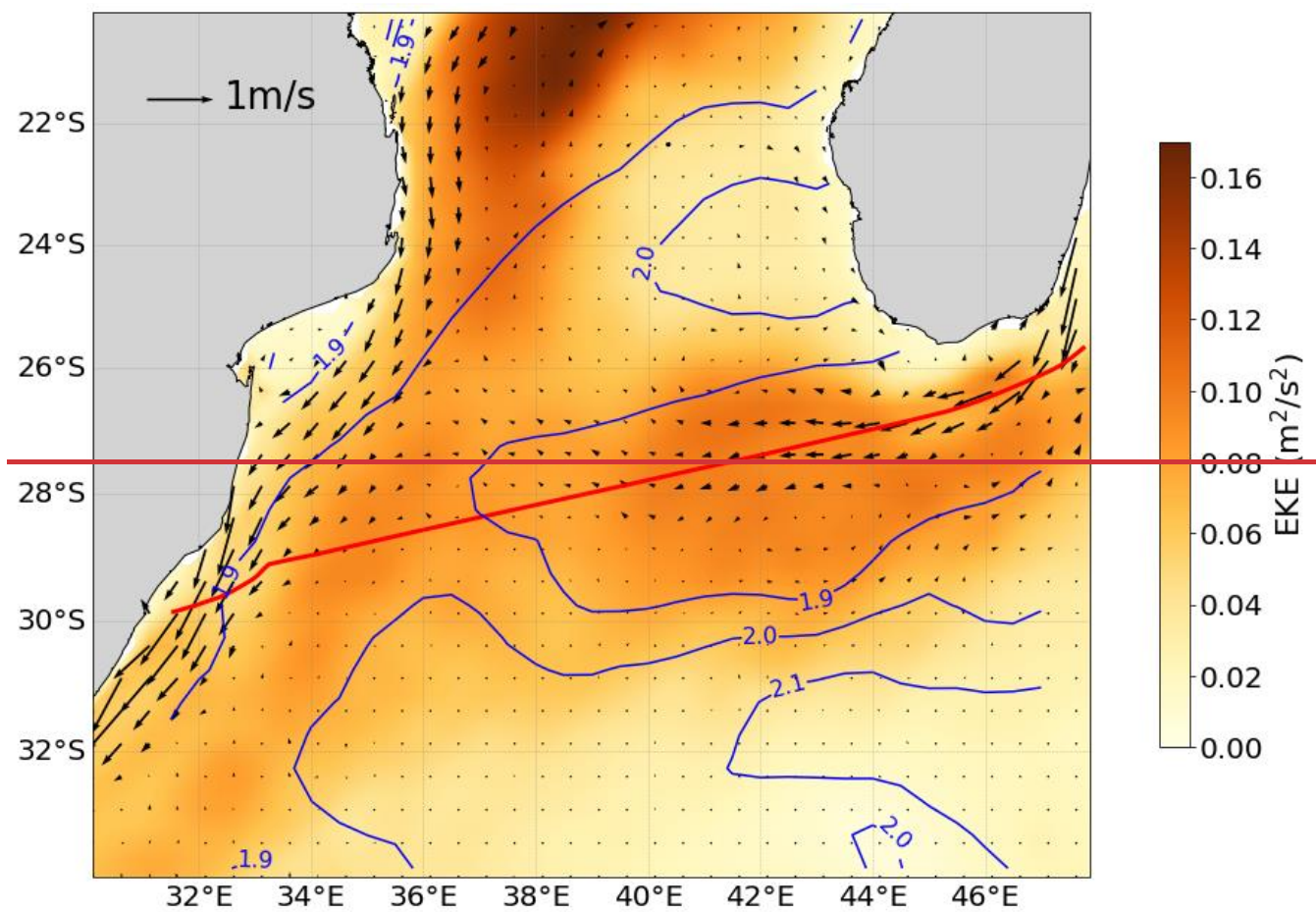
239
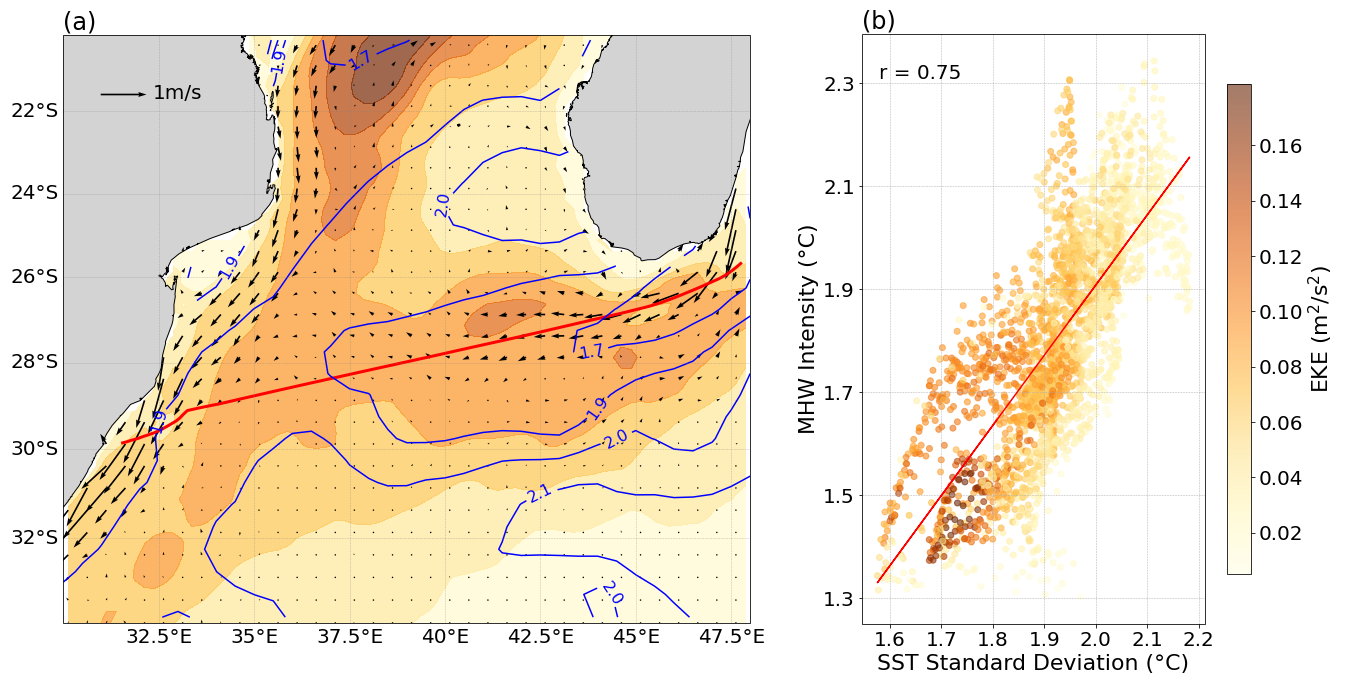
Figure 3: a) Mean eddy kinetic energy (EKE), with mean geostrophic velocities overlaid, calculated from high resolution AVISO data for the climatological period from 1993–2023. The blue contour lines indicate SST standard deviation (°C) calculated from NOAA optimally interpolated sea surface temperature (OISST V2) high resolution (0.25°) gridded SST data for the same period from 1993–2023. The red solid line denotes the IX21 XBT transect. **b)** Scatter plot of mean annual MHW Intensity (°C) and SST standard deviation (°C). Colours indicate the EKE at these points. The regression line (red) between MHW Intensity and SST standard deviation and the significant correlation coefficient are indicated. ~~Mean eddy kinetic energy (EKE), with mean geostrophic velocities overlaid, calculated from high resolution AVISO data for the climatological period from 1993–2023. The blue contour lines indicate SST standard deviation (°C) calculated from NOAA optimally interpolated sea surface temperature (OISST V2) high resolution (0.25°) gridded SST data for the same period from 1993–2023. The red solid line denotes the IX21 XBT transect.~~

3.2 Subsurface temperature anomaly properties associated with surface–identified MHWs

To examine the subsurface signal of MHWs, we identified when surface MHWs (detected from SST satellite data) were both co–located with and occurred simultaneously along the IX21 XBT line. MHWs of varying intensities and sizes were identified in the SST data on 65 days with corresponding XBT transects. For each day and location where a MHW signal was present over the XBT transect, 92% experienced maximum temperature anomalies below the surface (0 m) and 68% of the subsurface warm anomaly profiles (associated with the presence of MHWs), extended down to 800 m.

A significant relationship was found between surface temperature anomalies and maximum subsurface anomalies ($r = 0.70$, p–value < 0.0001), as subsurface anomalies tend to increase with increasing surface anomalies (Fig. 4a). Furthermore, deeper MHW events (depth of subsurface anomaly maxima > 500 m) tend to experience stronger subsurface anomalies than shallower events in the upper 200 m where surface and subsurface anomalies are more comparable (Fig. 4a). This observed depth–

261 dependent pattern suggests that the depth of the subsurface warm anomaly may play a role in modulating subsurface thermal
262 responses to surface anomalies.

263 According to the distribution of surface and subsurface anomalies, there is a significant difference between the surface and
264 subsurface anomalies (p–value < 0.001) (Fig. 5b). Subsurface anomalies are, on average, 1.04 °C warmer than the anomalies
265 at the surface and experience a larger range of warmer temperatures than that of surface anomalies (Fig. 4b). These differences
266 in mean values and variability indicate that temperature anomalies, associated with surface MHWs, intensify below the surface.

267
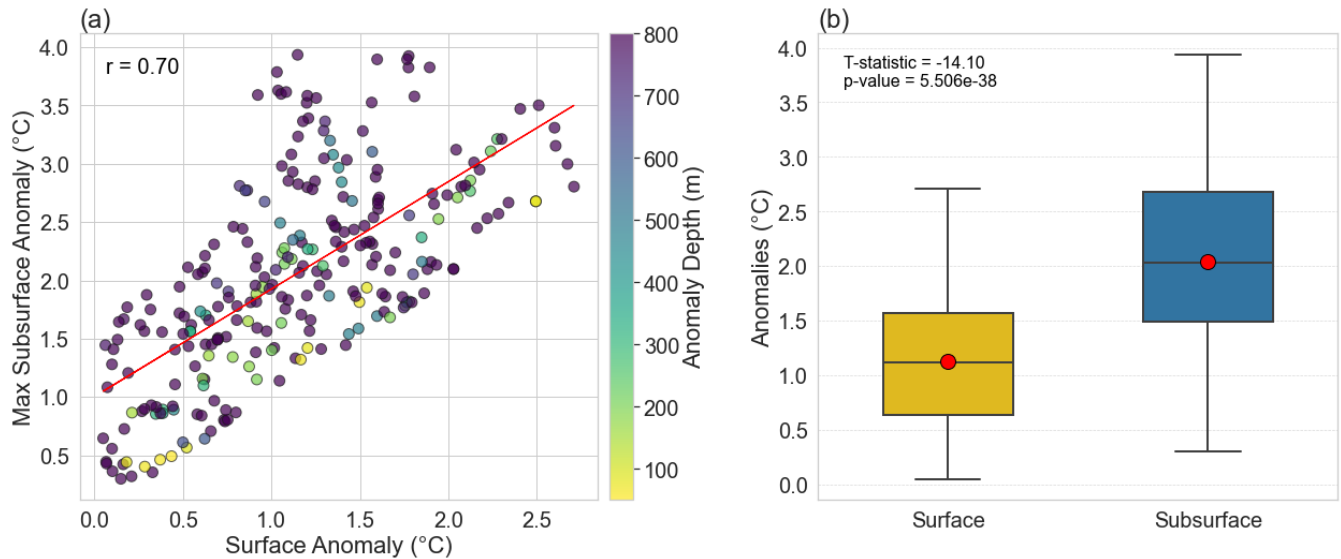
268 **Figure 4: a)** Scatter plot of surface anomalies and maximum subsurface anomalies at points where surface MHWs were identified. Colours
269 indicate the maximum depth of warm temperature anomalies. The regression line (red) between surface and subsurface anomalies
270 and correlation coefficient are indicated. **b)** Boxplot comparing surface and subsurface anomalies. Red markers indicate mean values, while
271 the central line shows the median. Boxes represent the interquartile range (IQR), with whiskers extending to 1.5 times the IQR. T–statistic
272 and p–value from a two–sample t–test are displayed, highlighting the significance of the difference.

273 To further explore subsurface intensification of the temperature anomaly signals associated with MHWs, the relationship
274 between maximum subsurface temperature anomalies (°C) and their corresponding depths (m) was evaluated in relation to sea
275 level anomalies (SLA) (Fig. 5). A positive, statistically significant relationship between maximum subsurface anomaly
276 temperature is found, with a correlation of 0.5 (p–value < 0.0001), showing that the warmest subsurface temperatures are
277 typically associated with greater depths (Fig. 6a). This highlights a positive association between the magnitude of the
278 subsurface temperature anomaly and the depth at which it occurs and points to an underlying physical or environmental
279 mechanism linking these variables.

280 Since the SWIO is an eddy–dominated region, the influence of mesoscale eddies on the depth of maximum subsurface
281 anomalies is investigated. The majority of the subsurface temperature anomaly profiles are associated with anti–cyclonic
282 eddies, with 78.62% of the profiles associated with positive SLA (Fig. 5a). These subsurface maximum temperature anomalies
283 occur at depths ranging from 0–270 m, whereas profiles associated with cyclonic eddies experience maximum temperature

anomaly depths ranging from 0–60 m, with two outliers extending to depths of 170 m and 180 m (Fig. 5b). Furthermore the mean maximum subsurface anomaly associated with anti–cyclonic eddies (positive SLA) is significantly deeper than the mean maximum subsurface anomaly depth associated with cyclonic eddies (p–value < 0.0001), with mean depths of 100 m and 51 m respectively (Fig 5b). This highlights the significant role of mesoscale eddies in shaping the vertical distribution of subsurface temperature anomalies in the SWIO, with anti–cyclonic eddies driving temperature anomalies to greater depths compared to the shallower depths associated with cyclonic eddies.
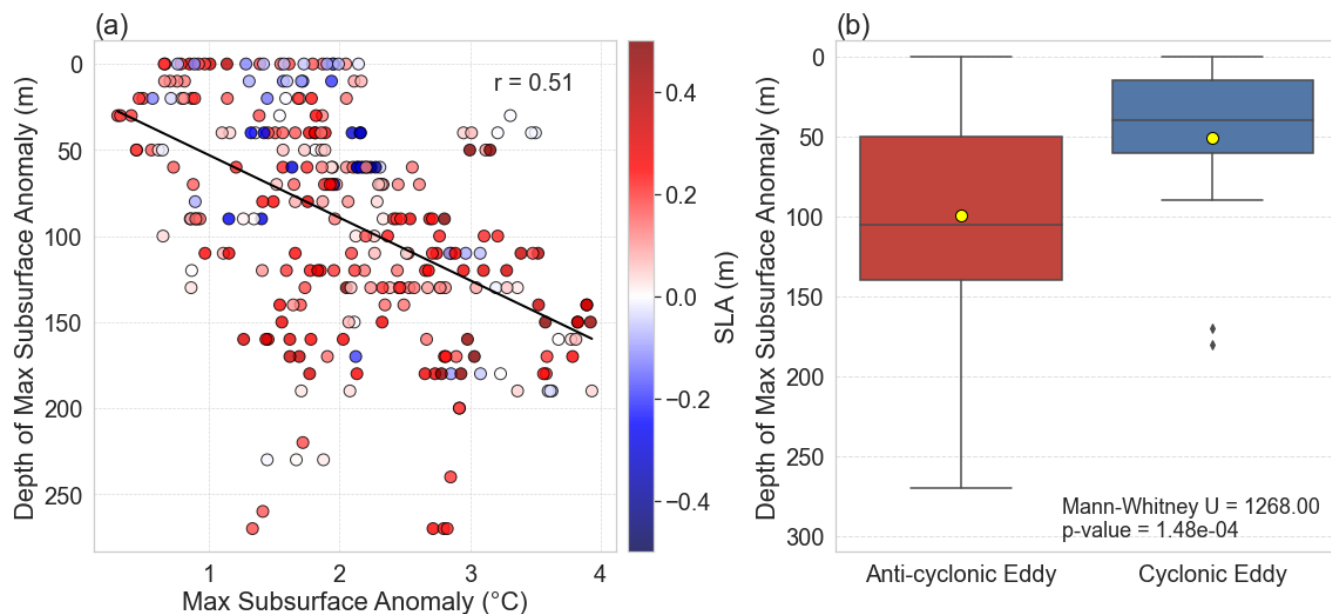
Figure 5: a) Scatterplot showing the relationship between maximum subsurface temperature anomalies (°C) and their corresponding depths (m), color–coded by Sea Level Anomalies (SLA, m). Positive SLA values (red) indicate anti–cyclonic eddies, while negative SLA values (blue) represent cyclonic eddies. **b)** Boxplot comparing the depths of maximum subsurface anomalies between anti–cyclonic and cyclonic eddies. Yellow markers indicate mean values, while the central line shows the median. Boxes represent the interquartile range (IQR), with whiskers extending to 1.5 times the IQR. Mann–Whitney U and p–value from a two–sample t–test are displayed, highlighting the significance of the difference.

~~The IX21 transect, used in this study to extrapolate *in situ* subsurface data and investigate the subsurface extent of MHWs, runs through the SEMC leakage and across the source region of the AC, where eddy activity is high and geostrophic currents are strong (Fig. 3). Thus, when investigating the subsurface structure of MHWs along the XBT line, we may capture MHW events that are driven by mesoscale eddy activity and occur frequently, but have reduced annual duration, intensity and cumulative intensity, compared to the rest of the region.~~

3.3.1 Case studies of MHW events in the SWIO and their subsurface manifestation~~Annual and seasonal surface MHW variability~~

Given the statistically significant relationship between surface MHW signals and subsurface temperature anomalies, as well as the depth–dependent structure of these anomalies in relation to mesoscale eddies, three surface–identified MHW events (9 January 2020, 14 July 2012 and 20 October 2007) were selected as case studies. These events, which persisted over the IX–

307   21 XBT transect, were analysed to further investigate their spatial and subsurface characteristics in the SWIO (Fig. 6). To

308   investigate the subsurface signal of MHWs, we identified when the surface MHWs detected in the SST satellite data were co-

309   located with the IX21 XBT line. 65 MHWs of varying intensities and sizes were identified in the SST data on days with

310   corresponding XBT transects. For each day where subsurface data was available and a MHW signal was present over the

311   XBT transect, the surface MHW intensity was compared to daily subsurface temperature and anomaly profiles. MHWs that

312   occurred on 9 January 2020, 14 July 2012 and 20 October 2007 were selected as case studies (Fig. 4).

313   For all three case studies, the spatial distribution of the MHWs are aligned with the spatial distribution of the warm–core

314   anticyclonic eddies, with maximum MHW intensities directly surrounding the cores of the largest anticyclonic eddies (Fig.

315   6a–d). For example, for the 9 January 2020 MHW case study, the maximum MHW intensities (2.5 °C) are identified

316   surrounding the largest anticyclonic, with warm core eddies of 0.5 m above sea level, at 27–32° S and 36–42° E (Fig. 6a and

317   d). Likewise, on 14 July 2012 and 20 October 2007, the most intense surface MHW temperatures were recorded (2 °C and 1.5

318   °C, respectively) surrounding the largest sea level anomalies (0.4–0.5 m above sea level) (Fig. 6b,c,e and f).

319

320
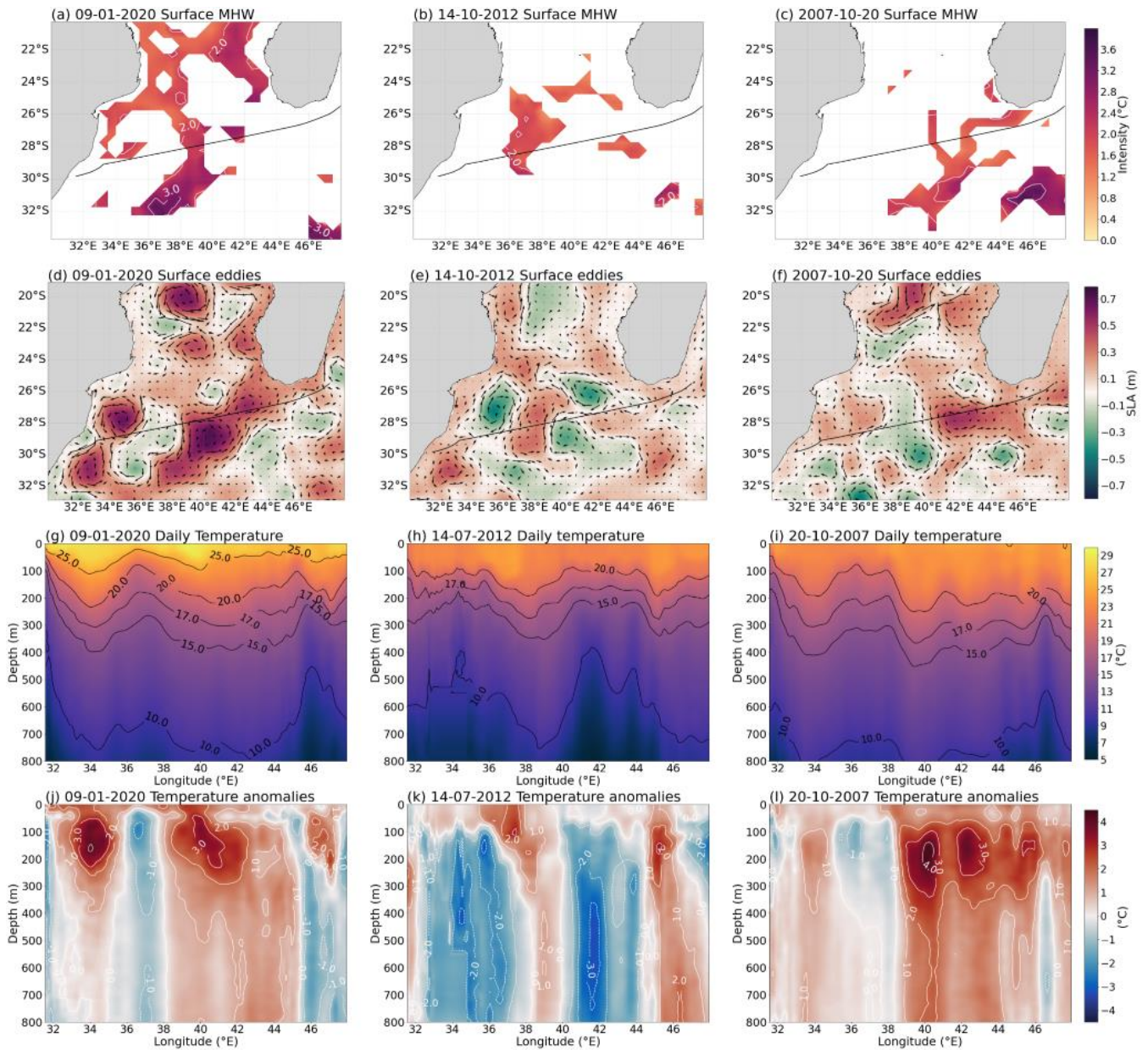
Figure 64: Surface MHW intensity using OISST V2 data (°C) that took place on **(a)** 9 January 2020, **(b)** 14 July 2012, **(c)** 20 October 2007. Sea level anomalies (m) and geostrophic current velocities (m/s) on the three MHW case study days **(d)** 9 January 2020, **(e)** 13 July 2012 and **(f)** 20 October 2007 using optimally interpolated AVISO altimetry satellite data. The black solid line indicates the position of the XBT transect (IX21). Subsurface temperature **(g – i)** and temperature anomalies **(j – l)** from the 9th – 13th January 2020 **(g and j)**, the 14th – 17th July 2012 **(h and k)** and the 20th – 24th October 2007 **(i and l)**. The subsurface profiles are from *in situ* XBT data from the IX21 transect line (see methods section). ~~Surface MHW intensity using OISST V2 data (°C) that took place on **(a)** 9 January 2020, **(b)** 14 July 2012, **(c)** 20 October 2007. Sea level anomalies (m) and geostrophic current velocities (m/s) on the three MHW case study days **(d)** 9 January 2020, **(e)** 20 October 2007 and **(f)** 13 July 2012 using optimally interpolated AVISO altimetry satellite data. The black solid line indicates the position of the XBT transect (IX21). Subsurface temperature **(g - i)** and temperature anomalies **(j - l)** from the 9th – 13th January 2020 **(g and j)**, the 14th – 17th July 2012 **(h and k)** and from the 20th – 24th October 2007 **(i and l)**. The subsurface profiles were plotted using in situ XBT data from the IX21 transect line (see methods section).~~

333

Moreover, anomalously warm temperatures surrounding warm–core eddies are present with depth at the locations where MHWs persist over the XBT transect line (Fig. 6a–c and g–l). During the January 2020 MHW event, two distinct columns of anomalously warm temperatures (1–4 °C) extend from the surface to 800 m at 34° E and 38–45° E (Fig. 6j). At 36–38° E, the location of the surface–identified July 2012 MHW, anomalously warm water (1–2 °C) extends from the surface to 800 m (Fig. 6h). Between 39–46° E, the October 2007 MHW has temperature anomalies (1–4 °C) that extend below the surface–identified MHW to 800 m (Fig. 6l).

The subsurface temperature anomalies associated with surface–identified MHWs, intensify below the surface (Fig. 6a,b,c,j,k,l and Table 1). During the January 2020 MHW case study, the subsurface temperature anomalies, relative to the surface MHW intensity (2.5 °C) at 34° E and between 38–45° E, are most extreme from 50–200 m, reaching up to 4 °C (Fig. 6a and j and Table 1). Similarly, subsurface temperature anomalies during the October 2007 MHW event reach maximum temperatures (4°C) above the seasonal mean below 100 m at 40° E, 42° E and 45° E (Fig. 6l and Table 1). Although much weaker, at 38° E, the subsurface temperature anomaly that extends below the surface–identified July 2012 MHW has a maximum anomaly of 2 °C that extends from 0–150 m (Fig. 6k and Table 1). Given that the mixed layer depth, on average, in this region does not exceed 100 m (de Boyer Montégut et al., 2004), the most intense MHW temperatures are experienced below the mixed layer, and not at the surface.

Table 1: Surface and subsurface MHW characteristics for all three case studies: location of surface MHW over XBT transect (Location), temperature anomalies (maximum surface intensity ('Max. Surface'), maximum temperature anomaly ('Max. subsurface') and the depth where it occurs ('Depth of Max.')), SLA at the location of surface–identified MHWs (SLA) where positive indicates the presence of a warm core eddy.

MHW case studies	Location	Temperature anomalies			SLA (m)
		Max. Surface (°C)	Max. Subsurface (°C)	Depth of Max. (m)	
09–01–2020	34° E; 38–45° E	2.5	4	100–200	0.5
14–07–2012	36–38° E	2	2	100	0.2
20–10–2007	39–46° E	1.5	4	100–200	0.4

353

However, weaker subsurface temperature anomalies are associated with warm–core eddies where there is no surface identified MHW signal (Fig. 6a–l). At 46° E, during both the January 2020 and July 2012 MHW case studies, a weak subsurface

temperature anomaly (1–2°C) extends below the surface where no surface MHW was identified, but a warm–core mesoscale eddy (SLA of 0.2–0.4 m) is found (Fig. 6 a,b, j and k). Similarly, between 32 – 36° E during the October 2007 MHW, a weak column of anomalously warm water (1–2 °C) extends from 0–800 m and is associated with an eddy (SLA of 0.3 m) rather than a surface identified MHW (Fig. 6c, f and l). Nonetheless, the most extreme subsurface temperature anomalies strongly reflect the vertical extent of the surface MHW, rather than a warm core eddy signature, as the anomalies associated with surface identified MHWs and mesoscale eddies are larger than those associated with mesoscale eddies alone (Fig. 6a–c and g–l). Overall, the three MHW case studies have different spatial distributions and intensities, but there are several commonalities between all three events (Fig. 6). All three case studies indicate that MHWs are associated with warm–core anticyclonic eddies and subsurface temperature anomalies that extend down to at least 800 m and intensify below the surface typically within the thermocline.

4. Discussion

Our study reveals distinct spatial patterns in the surface and subsurface extent of MHW characteristics within the SWIO and emphasizes the critical role of mesoscale eddies in shaping both surface and subsurface anomalies. The subsurface intensification of surface–identified MHW signals, which is modulated by mesoscale processes, highlights the importance of understanding the subsurface dynamics when assessing MHW impacts and underscores the importance of an integrated approach to studying MHW variability in this region.

On average, the range of the mean annual surface MHW metrics (frequency, intensity, duration and cumulative intensity) are considered typical for highly dynamic WBCs systems and are classified as intense and abrupt events (Oliver et al., 2018; Holbrook et al., 2019; Marin et al., 2022). However, across the SWIO, MHW metrics exhibit distinct spatial distributions which are linked to the underlying patterns of SST variability and mesoscale eddy activity. These regional differences of MHW characteristics are likely driven by the local processes that drive SST variability and the variable circulation itself (Oliver et al., 2018).

In particular, areas of low SST variance are characterized by more frequent, less intense and shorter events, whereas areas of high SST variance have less frequent MHW events but they are more intense and longer lasting. The regions of low SST variance fall within the main passageway of the eddies through the MC and from the SEMC leakage into the AC source region. Here, less intense but frequent MHWs are expected and found in our study, as these are typical characteristics of MHWs in WBCs where the high abundance of rapidly propagating eddies is known to dictate the growth and decay of MHWs (Frölicher et al., 2018; Oliver et al., 2018; Oliver, 2019; Spillman et al., 2021; Fragkopoulou et al., 2023). Since the IX21 XBT transect runs through the region of high eddy activity, our results capture the subsurface anomalies associated with MHW events that are influenced by mesoscale eddy activity and occur frequently, but have reduced annual duration, intensity and cumulative intensity, compared to the rest of the region.

Moreover, mesoscale eddies play a critical role in shaping the depth of subsurface temperature anomalies associated with surface MHWs. Distinct columns of deep, anomalously warm temperatures were located below surface–identified MHWs. The majority of the subsurface anomalies associated with MHWs extend to depths down to 800m, with maximum temperature anomalies occurring beneath the surface. Surface temperature anomalies are correlated with their associated maximum subsurface temperature anomalies as well as the depth of the subsurface anomalies, meaning that more intense MHWs experience deeper and warmer maximum subsurface anomalies. Specifically, anti–cyclonic warm–core eddies are associated with much deeper maximum subsurface anomalies. This is observed during all three case studies, where the MHWs persist within anti–cyclonic eddies that vary in magnitude. The more intense 2007 and 2020 MHWs experience much stronger and deeper maximum subsurface temperature anomalies, associated with stronger anti–cyclonic eddies, compared to the 2012 MHW subsurface temperature anomaly, associated with a weaker anti–cyclonic eddy. This further demonstrates that, as is seen in other WBCs, anomalously warm anticyclonic eddies may act as a mechanism for MHW intensification below the surface (Schaeffer and Roughan, 2017; Elzahaby et al., 2021; Mawren et al., 2022 a; Azarian et al., 2024) (Schaeffer and Roughan, 2017; Elzahaby and Schaeffer, 2019; Elzahaby et al., 2021; Perez et al., 2021; Amaya et al., 2023; Fragkopoulou et al., 2023; Azarian et al., 2024). Furthermore intensification of warm–core eddies, under the current WBC warming trends, may subsequently amplify MHW events and intensify their subsurface signals in the future (Wu et al., 2012; Schaeffer and Roughan, 2017; Benthuysen et al., 2020). This growing influence of mesoscale eddies on subsurface MHWs, under ongoing global warming, may be driven by the faster response of the mixed layer compared to the slower response of the deep ocean, which affects the vertical distribution of heat and emphasizes the value of considering vertical structures in future ocean warming studies (Zhang et al., 2023; Azarian et al., 2024; He et al., 2024).

Since regions with high eddy abundance are likely to experience a large proportion of deep, subsurface–intensified MHWs, the exposure of vital coastal ecosystems to these events may be significantly underestimated when MHWs are studied using satellite data alone (Elzahaby & Schaeffer, 2019; Fragkopoulou et al., 2023). This underestimation is particularly concerning in the SWIO, where MHWs have previously been linked to severe coral bleaching events, such as the extreme bleaching of Le Grand Récif de Toliara, one of the largest and most biodiverse barrier reef systems (Mawren et al., 2022a). In addition, the co–occurrence of MHWs and tropical cyclones in the SWIO exacerbates their impacts, as cyclones can intensify MHW events, leading to more severe thermal stress. These combined phenomena have had devastating consequences for coastal marine ecosystems, particularly off southeastern Africa, where frequent and intense MHWs have triggered severe coral bleaching (Mawren et al., 2022b). Damage to habitat–forming coral species initiates cascading effects on marine ecosystems, threatening biodiversity and fisheries that are essential to the livelihoods of coastal communities in Madagascar and surrounding regions (Obura, 2012; Pereira et al., 2014; Obura et al., 2021; Mawren et al., 2022b). This highlights the importance of examining subsurface MHW signals, as satellite–based analyses alone may overlook the full extent of the thermal stress and ecological consequences for mesopelagic fishes, including changes in prey availability for deep–diving predators (Iglasias et al., 2024). It should be noted, however, that although mesoscale eddies do influence the subsurface characteristics of anomalies associated with MHWs, past heat budget studies of global MHWs have shown that abrupt and intense MHWs are likely driven by a

combination of processes, such as local advection, eddy heat flux, air–sea heat flux and large–scale climate modes, which control heat variations over various spatio–temporal scales (Hayashida et al., 2020; Marin et al., 2022). The complexity of the SWIO therefore suggests that it is likely a combination of different oceanic and atmospheric processes that drive MHWs and warrant further investigation. Ultimately, this will enhance our understanding of subsurface biological impacts and inform management strategies aimed at preventing irreversible damage to ocean ecosystems. MHWs in the SWIO can be classified as abrupt and intense events, which is typical for highly dynamic WBCs (Marin et al., 2022). Regions with annual maximum MHW cumulative intensity, which is the integration of MHW duration and intensity, experience the most severe impacts on marine ecosystems (Holbrook et al., 2020). Southwest of Madagascar, where maximum cumulative intensity is observed, MHWs have previously caused severe coral bleaching events in one of the largest barrier reef coral systems, Le Grand Recif Toliara (Mawren et al., 2022 a). Furthermore, the co–occurrence of MHWs and tropical cyclones across the SWIO causes these extreme events to intensify, which has not only had devastating impacts on southeast African coastal countries and Madagascar, but has also severely impacted coastal marine ecosystems, especially through the exacerbation of coral bleaching events off the southeast African coast, where this study showed MHWs are frequent and intense (Mawren et al., 2022 b). This highlights the importance of studying MHWs in this region as damage to habitat–forming coral species may have cascading impacts on the entire structure and functioning of the marine ecosystem, which upholds high marine biodiversity and supports fisheries largely depended upon by the coastal community of Madagascar (Obura, 2012; Pereira et al., 2014; Obura et al., 2021; Mawren et al., 2022 b).

In the SWIO, regions with high eddy activity and lower SST variability experience MHWs that occur frequently, but are shorter lived and less intense, whereas regions with low eddy activity, but high SST variability, experience more intense, longer lasting, but less frequent MHWs. Less intense and shorter–lived MHWs are typical of WBCs with high eddy abundance (Frölicher et al., 2018; Oliver et al., 2018; Oliver, 2019; Spillman et al., 2021; Fragkopoulou et al., 2023). The passage of eddies through the MC and from the SEMC largely dictates the growth and decay of MHWs in the SWIO (Bian et al., 2023; Zhang et al., 2023). On the other hand, more intense, longer lasting, but less frequent MHWs occur where SST variability is high, but eddy activity is low and weak surface currents are present. The local processes that drive high SST variability are known to result in more intense MHWs (Oliver et al., 2018). Since MHWs within WBCs predominantly occur within warm–core anticyclonic eddies, weak mean flow and high eddy injection southwest of Madagascar and in the region of SEMC retroflection likely drives higher mean SST variability which establishes, on average, more intense MHWs (Halo et al., 2014). However, other processes, such as anomalous net surface heat fluxes driven by weaker winds and increased insolation may also play a role in driving higher SST variability, and thus more intense MHWs, in these regions (Mawren et al., 2022 a). Furthermore, the presence of mesoscale eddies surrounding surface MHWs during the three selected case studies indicates that, as is seen in other WBCs, anomalously warm anticyclonic eddies act as a mechanism for MHW intensification (Schaeffer and Roughan, 2017; Elzahaby et al., 2021; Mawren et al., 2022 a). During the case studies, greatest MHW intensity was present where anomalously high SLA that exceeded the mean SLA amplitudes (0.3 cm) generally associated with warm–core eddies in SWIO (Schouten et al., 2003; Swart et al., 2010; Halo et al., 2014). This is significant as WBC systems and their dynamical

processes, such as mesoscale eddies, are intensifying and causing WBC warming to be two to three times faster than the mean global ocean warming rate (Wu et al., 2012). Intensification of warm core eddies, under the current WBC warming trends, may subsequently intensify local SST variability and amplify MHW events in the future (Wu et al., 2012; Schaeffer and Roughan, 2017; Benthuysen et al., 2020).

The intensification of MHWs in the presence of mesoscale eddies is not limited to the surface, as distinct columns of deep-reaching and warm temperature anomalies are identified below the surface-identified MHW case studies. Eddies in the SWIO, can extend to intermediate depths of 800 - 2000m (Quartly and Srokosz, 2004; Halo et al., 2014). We found that subsurface temperature anomalies associated with MHWs in the SWIO could extend to at least 800m below surface detected MHWs. Furthermore, the observed temperature anomalies intensify below the surface, and reach temperatures which exceed the surface MHW intensities below the MLD, which could also be associated with a deepening of the thermocline (Schaeffer and Roughan, 2017; Elzahaby and Schaeffer, 2019; Amaya et al., 2023; Fragkopoulou et al., 2023). This suggests that, as is seen in other WBCs where eddies drive deeper and longer-lasting MHWs, anticyclonic eddies may restrict the horizontal extent of MHWs in the SWIO and also act to localise the intensity of the MHW within the eddy column, below the surface (Schaeffer and Roughan, 2017; Elzahaby and Schaeffer, 2019; Elzahaby et al., 2021; Perez et al., 2021; Fragkopoulou et al., 2023; Zhang et al., 2023). These findings highlight the importance of studying the subsurface extent of MHWs, as exposure of vital coastal ecosystems to the effects of MHWs may be largely underestimated when only studying MHWs using surface satellite data (Schaeffer and Roughan, 2017; Elzahaby and Schaeffer, 2019; Benthuysen et al., 2020; Elzahaby et al., 2021; Zhang et al., 2023).

Overall, we find that mesoscale eddies not only play an important role in dictating the frequency, duration and intensity of surface MHW events, but the subsurface temperature anomalies also extend below a surface-identified MHW. Thus, the importance of mesoscale eddies in driving MHW extents in the SWIO is highlighted. However, past heat budget studies of global MHWs using high-resolution models (Hayashida et al., 2020; Marin et al., 2022) have shown that abrupt and intense MHWs are likely driven by a mixed combination of processes, such as local advection, eddy heat flux, air-sea heat flux and large-scale climate modes, which control heat variations over small and different spatio-temporal scales. The high complexity of the SWIO therefore suggests that, while eddies may act as a catalyst for MHW events, it is likely a combination of different oceanic and atmospheric processes that drive MHWs, which warrant further investigation.

5. Conclusions

To date, our study is the first to describe the subsurface extent of MHWs in the Greater Agulhas Current System, the WBC of the SWIO. Furthermore, the distinct spatial patterns in the surface and subsurface extent of MHW characteristics emphasize the critical influence of mesoscale eddies in shaping these thermal anomalies. The strong relationship between surface MHW signals and subsurface temperature anomalies highlights the importance of considering subsurface dynamics when assessing MHW impacts. By analyzing case studies of persistent MHW events, we demonstrate how mesoscale processes modulate both

the intensity and vertical structure of these anomalies, underscoring the need for an integrated approach to studying MHW variability in this region This finding demonstrates that investigation of MHWs using only surface satellite data may significantly underestimate the severity and impacts of MHWs. The presence of anticyclonic warm–core eddies influences both the surface distribution and subsurface signals of MHWs, in particular their depth extent. ~~To date, our study is the first to describe the subsurface extent of MHWs in the Greater Agulhas Current System, which makes up the SWIO, and reveals that these events can extend to depths of at least 800 m and exhibit maximum intensity below the surface. This finding suggests that investigation of MHWs using only surface satellite data may significantly underestimate the severity and impacts of MHWs. The presence of anticyclonic warm core eddies appears to influence both the surface distribution and subsurface signals of MHWs, indicating a complex interaction that warrants further investigation.~~

Our results highlight the need for consistent and long-term subsurface data to better understand the progression, frequency, and duration of MHWs below the surface. Investigating heat budgets and the drivers of MHWs will provide deeper insights into the mechanisms behind these events, enhancing the accuracy of forecasting models and improving management strategies to mitigate the impacts on marine ecosystems.

Future research should prioritize specific locations within the SWIO where MHWs are most extreme or frequent, focusing on areas with high marine biodiversity, such as coral reef systems. These targeted studies will be crucial for understanding local MHW characteristics and their effects on fisheries and coastal economies, ultimately contributing to more effective conservation and resource management efforts.

Code availability

The code used to detect MHWs is available at https://github.com/ecjoliver/marineHeatWaves.

Data availability

All data used in this study are open access. The daily NOAA OISST V2 data is available at https://coastwatch.pfeg.noaa.gov/erddap/ (Huang et al., 2020). The HR-XBT data is made available by the Scripps Institution of Oceanography HR-XBT program (IX21 - http://www-hrx.ucsd.edu/ix15.html) The AVISO product is available from CMEMS (https://doi.org/10.48670/moi-00148, E.U. CMEMS).

Author contributions

CBW performed the analysis and led the writing of the manuscript ~~as part of her Honours research project~~ at University of Cape Town, South Africa. JCS, JS, TM, DM and NM supervised, proposed and guided the project, and contributed to ~~the~~ writing and analysis.

Competing interests

The authors declare that they have no conflict of interest.

Disclaimer

Acknowledgements

The research leading to these results has received funding from the National Research Foundation (NRF) through Grant PMDS230630125138, the South African Environmental Observation Network (SAEON) and the University of Cape Town. JS was supported by the NOAA Global Ocean Monitoring and Observing Program through Award NA20OAR4320278. NM was supported by Australian Research Council Future Fellowship FT220100475.

References

Amaya, D. J., Jacox, M. G., Alexander, M. A., Scott, J. D., Deser, C., Capotondi, A., and Phillips, A. S.: Bottom marine heatwaves along the continental shelves of North America, Nat. Commun., 14, 1038, https://doi.org/10.1038/s41467-023-36567-0, 2023.

Azarian, C., Bopp, L., Pietri, A., Sallée, J.–B., and d'Ovidio, F.: Current and projected patterns of warming and marine heatwaves in the Southern Indian Ocean, Progress in Oceanography, 215, 103036, https://doi.org/10.1016/j.pocean.2023.103036, 2023.

Bai, L., Zhu, G., Huang, H., Zhang, L., Lü, H., and Zhang, Y.: Characteristics of mesoscale eddies in the Mozambique Channel, PLOS ONE, 19, e0302367, https://doi.org/10.1371/journal.pone.0302367, 2024.

Banzon, V., Smith, T. M., Chin, T. M., Liu, C., and Hankins, W.: A long-term record of blended satellite and in situ sea-surface temperature for climate monitoring, modeling and environmental studies, Earth Syst. Sci. Data, 8, 165–176, https://doi.org/10.5194/essd-8-165-2016, 2016.

Beal, L. M., De Ruijter, W. P. M., Biastoch, A., Zahn, R., SCOR/WCRP/IAPSO Working Group 136, Cronin, M., Hermes, J., Lutjeharms, J., Quartly, G., Tozuka, T., Baker-Yeboah, S., Bornman, T., Cipollini, P., Dijkstra, H., Hall, I., Park, W., Peeters,

F., Penven, P., Ridderinkhof, H., and Zinke, J.: On the role of the Agulhas system in ocean circulation and climate, Nature, 472, 429–436, https://doi.org/10.1038/nature09983, 2011.

Beal, L. M., Vialard, J., Roxy, M. K., Li, J., Andres, M., Annamalai, H., Feng, M., Han, W., Hood, R., Lee, T., Lengaigne, M., Lumpkin, R., Masumoto, Y., McPhaden, M. J., Ravichandran, M., Shinoda, T., Sloyan, B. M., Strutton, P. G., Subramanian, A. C., Tozuka, T., Ummenhofer, C. C., Unnikrishnan, A. S., Wiggert, J., Yu, L., Cheng, L., Desbruyères, D. G., and Parvathi, V.: A Road Map to IndOOS-2: Better Observations of the Rapidly Warming Indian Ocean, Bull. Am. Meteorol. Soc., 101, E1891–E1913, https://doi.org/10.1175/BAMS-D-19-0209.1, 2020.

Benthuysen, J. A., Oliver, E. C. J., Chen, K., and Wernberg, T.: Editorial: Advances in Understanding Marine Heatwaves and Their Impacts, Front. Mar. Sci., 7, 147, https://doi.org/10.3389/fmars.2020.00147, 2020.

Bian, C., Jing, Z., Wang, H., Wu, L., Chen, Z., Gan, B., and Yang, H.: Oceanic mesoscale eddies as crucial drivers of global marine heatwaves, Nat. Commun., 14, 2970, https://doi.org/10.1038/s41467-023-38811-z, 2023.

Chandler, M., Zilberman, N. V., and Sprintall, J.: Seasonal to Decadal Western Boundary Current Variability From Sustained Ocean Observations, Geophys. Res. Lett., 49, e2022GL097834, https://doi.org/10.1029/2022GL097834, 2022.

Chauhan, A., Smith, P. A. H., Rodrigues, F., Christensen, A., St. John, M., and Mariani, P.: Distribution and impacts of long-lasting marine heat waves on phytoplankton biomass, Front. Mar. Sci., 10, 1177571, https://doi.org/10.3389/fmars.2023.1177571, 2023.

Collins, C., Reason, C. J. C., and Hermes, J. C.: Scatterometer and reanalysis wind products over the western tropical Indian Ocean, J. Geophys. Res. Oceans, 117, 2011JC007531, https://doi.org/10.1029/2011JC007531, 2012.

DiMarco, S. F., Chapman, P., and Nowlin, W. D.: Satellite observations of upwelling on the continental shelf south of Madagascar, Geophys. Res. Lett., 27, 3965–3968, https://doi.org/10.1029/2000GL012012, 2000.

Elzahaby, Y. and Schaeffer, A.: Observational Insight Into the Subsurface Anomalies of Marine Heatwaves, Front. Mar. Sci., 6, 745, https://doi.org/10.3389/fmars.2019.00745, 2019.

Elzahaby, Y., Schaeffer, A., Roughan, M., and Delaux, S.: Oceanic Circulation Drives the Deepest and Longest Marine Heatwaves in the East Australian Current System, Geophys. Res. Lett., 48, e2021GL094785, https://doi.org/10.1029/2021GL094785, 2021.

Fragkopoulou, E., Sen Gupta, A., Costello, M. J., Wernberg, T., Araújo, M. B., Serrão, E. A., De Clerck, O., and Assis, J.: Marine biodiversity exposed to prolonged and intense subsurface heatwaves, Nat. Clim. Change, 13, 1114–1121, https://doi.org/10.1038/s41558-023-01790-6, 2023.

Frölicher, T. L., Fischer, E. M., and Gruber, N.: Marine heatwaves under global warming, Nature, 560, 360–364, https://doi.org/10.1038/s41586-018-0383-9, 2018.

Garrabou, J., Gómez-Gras, D., Medrano, A., Cerrano, C., Ponti, M., Schlegel, R., Bensoussan, N., Turicchia, E., Sini, M., Gerovasileiou, V., Teixido, N., Mirasole, A., Tamburello, L., Cebrian, E., Rilov, G., Ledoux, J., Souissi, J. B., Khamassi, F., Ghanem, R., Benabdi, M., Grimes, S., Ocaña, O., Bazairi, H., Hereu, B., Linares, C., Kersting, D. K., La Rovira, G., Ortega, J., Casals, D., Pagès-Escolà, M., Margarit, N., Capdevila, P., Verdura, J., Ramos, A., Izquierdo, A., Barbera, C., Rubio-Portillo,

E., Anton, I., López-Sendino, P., Díaz, D., Vázquez-Luis, M., Duarte, C., Marbà, N., Aspillaga, E., Espinosa, F., Grech, D., Guala, I., Azzurro, E., Farina, S., Cristina Gambi, M., Chimienti, G., Montefalcone, M., Azzola, A., Mantas, T. P., Fraschetti, S., Ceccherelli, G., Kipson, S., Bakran-Petricioli, T., Petricioli, D., Jimenez, C., Katsanevakis, S., Kizilkaya, I. T., Kizilkaya, Z., Sartoretto, S., Elodie, R., Ruitton, S., Comeau, S., Gattuso, J., and Harmelin, J.: Marine heatwaves drive recurrent mass mortalities in the Mediterranean Sea, Glob. Change Biol., 28, 5708–5725, https://doi.org/10.1111/gcb.16301, 2022.

Goni, G. J., Sprintall, J., Bringas, F., Cheng, L., Cirano, M., Dong, S., Domingues, R., Goes, M., Lopez, H., Morrow, R., Rivero, U., Rossby, T., Todd, R. E., Trinanes, J., Zilberman, N., Baringer, M., Boyer, T., Cowley, R., Domingues, C. M., Hutchinson, K., Kramp, M., Mata, M. M., Reseghetti, F., Sun, C., Bhaskar Tvs, U., and Volkov, D.: More Than 50 Years of Successful Continuous Temperature Section Measurements by the Global Expendable Bathythermograph Network, Its Integrability, Societal Benefits, and Future, Front. Mar. Sci., 6, 452, https://doi.org/10.3389/fmars.2019.00452, 2019.

Großelindemann, H., Ryan, S., Ummenhofer, C. C., Martin, T., and Biastoch, A.: Marine Heatwaves and Their Depth Structures on the Northeast U.S. Continental Shelf, Front. Clim., 4, 857937, https://doi.org/10.3389/fclim.2022.857937, 2022.

Guo, X., Gao, Y., Zhang, S., Wu, L., Chang, P., Cai, W., Zscheischler, J., Leung, L. R., Small, J., Danabasoglu, G., Thompson, L., and Gao, H.: Threat by marine heatwaves to adaptive large marine ecosystems in an eddy-resolving model, Nat. Clim. Change, 12, 179–186, https://doi.org/10.1038/s41558-021-01266-5, 2022.

Halo, I., Backeberg, B., Penven, P., Ansorge, I., Reason, C., and Ullgren, J. E.: Eddy properties in the Mozambique Channel: A comparison between observations and two numerical ocean circulation models, Deep Sea Res. Part II Top. Stud. Oceanogr., 100, 38–53, https://doi.org/10.1016/j.dsr2.2013.10.015, 2014.

Hayashida, H., Matear, R. J., Strutton, P. G., and Zhang, X.: Insights into projected changes in marine heatwaves from a high-resolution ocean circulation model, Nat. Commun., 11, 4352, https://doi.org/10.1038/s41467-020-18241-x, 2020.

He, Q., Zhan, W., Feng, M., Gong, Y., Cai, S., & Zhan, H.: Common occurrences of subsurface heatwaves and cold spells in ocean eddies, Nature, 634, 1111–1117. https://doi.org/10.1038/s41586–024–08051–2, 2024.

Hermes, J. C., Masumoto, Y., Beal, L. M., Roxy, M. K., Vialard, J., Andres, M., Annamalai, H., Behera, S., D'Adamo, N., Doi, T., Feng, M., Han, W., Hardman-Mountford, N., Hendon, H., Hood, R., Kido, S., Lee, C., Lee, T., Lengaigne, M., Li, J., Lumpkin, R., Navaneeth, K. N., Milligan, B., McPhaden, M. J., Ravichandran, M., Shinoda, T., Singh, A., Sloyan, B., Strutton, P. G., Subramanian, A. C., Thurston, S., Tozuka, T., Ummenhofer, C. C., Unnikrishnan, A. S., Venkatesan, R., Wang, D., Wiggert, J., Yu, L., and Yu, W.: A Sustained Ocean Observing System in the Indian Ocean for Climate Related Scientific Knowledge and Societal Needs, Front. Mar. Sci., 6, 355, https://doi.org/10.3389/fmars.2019.00355, 2019.

Hobday, A. J. and Pecl, G. T.: Identification of global marine hotspots: sentinels for change and vanguards for adaptation action, Rev. Fish Biol. Fish., 24, 415–425, https://doi.org/10.1007/s11160-013-9326-6, 2014.

Hobday, A. J., Alexander, L. V., Perkins, S. E., Smale, D. A., Straub, S. C., Oliver, E. C. J., Benthuysen, J. A., Burrows, M. T., Donat, M. G., Feng, M., Holbrook, N. J., Moore, P. J., Scannell, H. A., Sen Gupta, A., and Wernberg, T.: A hierarchical approach to defining marine heatwaves, Prog. Oceanogr., 141, 227–238, https://doi.org/10.1016/j.pocean.2015.12.014, 2016.

Holbrook, N. J., Sen Gupta, A., Oliver, E. C. J., Hobday, A. J., Benthuysen, J. A., Scannell, H. A., Smale, D. A., and Wernberg, T.: Keeping pace with marine heatwaves, Nat. Rev. Earth Environ., 1, 482–493, https://doi.org/10.1038/s43017-020-0068-4, 2020.

Hu, S., Li, S., Zhang, Y., Guan, C., Du, Y., Feng, M., Ando, K., Wang, F., Schiller, A., and Hu, D.: Observed strong subsurface marine heatwaves in the tropical western Pacific Ocean, Environ. Res. Lett., 16, 104024, https://doi.org/10.1088/1748-9326/ac26f2, 2021.

Iglesias, I. S., Fiechter, J., Santora, J. A., and Field, J. C.: Vertical distribution of mesopelagic fishes deepens during marine heatwave in the California Current, ICES Journal of Marine Science, 81, 1837–1849, https://doi.org/10.1093/icesjms/fsae129, 2024.

Marin, M., Feng, M., Bindoff, N. L., and Phillips, H. E.: Local Drivers of Extreme Upper Ocean Marine Heatwaves Assessed Using a Global Ocean Circulation Model, Front. Clim., 4, 788390, https://doi.org/10.3389/fclim.2022.788390, 2022.

Mawren, D., Hermes, J., and Reason, C. J. C.: Marine heatwaves in the Mozambique Channel, Clim. Dyn., 58, 305–327, https://doi.org/10.1007/s00382-021-05909-3, 2022a.

Mawren, D., Hermes, J., and Reason, C. J. C.: Marine heat waves and tropical cyclones - Two devastating types of coastal hazard in South-eastern Africa, Estuar. Coast. Shelf Sci., 277, 108056, https://doi.org/10.1016/j.ecss.2022.108056, 2022a.

Mills, K., Pershing, A., Brown, C., Chen, Y., Chiang, F.-S., Holland, D., Lehuta, S., Nye, J., Sun, J., Thomas, A., and Wahle, R.: Fisheries Management in a Changing Climate: Lessons From the 2012 Ocean Heat Wave in the Northwest Atlantic, Oceanography, 26, https://doi.org/10.5670/oceanog.2013.27, 2013.

Obura, D.: The Diversity and Biogeography of Western Indian Ocean Reef-Building Corals, PLoS ONE, 7, e45013, https://doi.org/10.1371/journal.pone.0045013, 2012.

Obura, D., Gudka, M., Samoilys, M., Osuka, K., Mbugua, J., Keith, D. A., Porter, S., Roche, R., Van Hooidonk, R., Ahamada, S., Araman, A., Karisa, J., Komakoma, J., Madi, M., Ravinia, I., Razafindrainibe, H., Yahya, S., and Zivane, F.: Vulnerability to collapse of coral reef ecosystems in the Western Indian Ocean, Nat. Sustain., 5, 104–113, https://doi.org/10.1038/s41893-021-00817-0, 2021.

Oliver, E. C. J.: Mean warming not variability drives marine heatwave trends, Clim. Dyn., 53, 1653–1659, https://doi.org/10.1007/s00382-019-04707-2, 2019.

Oliver, E. C. J., Donat, M. G., Burrows, M. T., Moore, P. J., Smale, D. A., Alexander, L. V., Benthuysen, J. A., Feng, M., Sen Gupta, A., Hobday, A. J., Holbrook, N. J., Perkins-Kirkpatrick, S. E., Scannell, H. A., Straub, S. C., and Wernberg, T.: Longer and more frequent marine heatwaves over the past century, Nat. Commun., 9, 1324, https://doi.org/10.1038/s41467-018-03732-9, 2018.

Oliver, E. C. J., Benthuysen, J. A., Darmaraki, S., Donat, M. G., Hobday, A. J., Holbrook, N. J., Schlegel, R. W., and Sen Gupta, A.: Marine Heatwaves, Annu. Rev. Mar. Sci., 13, 313–342, https://doi.org/10.1146/annurev-marine-032720-095144, 2021.

Pereira, M., Litulo, C., Santos, R., Leal, M., Fernandes, R., Tibiriçá, Y., Williams, J., Atanassov, B., Carreira, F., Massingue, A., and Silva, I. M. D.: Mozambique marine ecosystems review, https://doi.org/10.13140/2.1.2092.5766, 2014.

Perez, E., Ryan, S., Andres, M., Gawarkiewicz, G., Ummenhofer, C. C., Bane, J., and Haines, S.: Understanding physical drivers of the 2015/16 marine heatwaves in the Northwest Atlantic, Sci. Rep., 11, 17623, https://doi.org/10.1038/s41598-021-97012-0, 2021.

Phillips, H. E., Tandon, A., Furue, R., Hood, R., Ummenhofer, C. C., Benthuysen, J. A., Menezes, V., Hu, S., Webber, B., Sanchez-Franks, A., Cherian, D., Shroyer, E., Feng, M., Wijesekera, H., Chatterjee, A., Yu, L., Hermes, J., Murtugudde, R., Tozuka, T., Su, D., Singh, A., Centurioni, L., Prakash, S., and Wiggert, J.: Progress in understanding of Indian Ocean circulation, variability, air–sea exchange, and impacts on biogeochemistry, Ocean Sci., 17, 1677–1751, https://doi.org/10.5194/os-17-1677-2021, 2021.

Quartly, G. D. and Srokosz, M. A.: Eddies in the southern Mozambique Channel, Deep Sea Res. Part II Top. Stud. Oceanogr., 51, 69–83, https://doi.org/10.1016/j.dsr2.2003.03.001, 2004.

Reynolds, R. W., Smith, T. M., Liu, C., Chelton, D. B., Casey, K. S., and Schlax, M. G.: Daily High-Resolution-Blended Analyses for Sea Surface Temperature, J. Clim., 20, 5473–5496, https://doi.org/10.1175/2007JCLI1824.1, 2007.

Roxy, M. K., Ritika, K., Terray, P., and Masson, S.: The Curious Case of Indian Ocean Warming, J. Clim., 27, 8501–8509, https://doi.org/10.1175/JCLI-D-14-00471.1, 2014.

Saranya, J. S., Roxy, M. K., Dasgupta, P., and Anand, A.: Genesis and Trends in Marine Heatwaves Over the Tropical Indian Ocean and Their Interaction With the Indian Summer Monsoon, J. Geophys. Res. Oceans, 127, e2021JC017427, https://doi.org/10.1029/2021JC017427, 2022.

Scannell, H. A., Johnson, G. C., Thompson, L., Lyman, J. M., and Riser, S. C.: Subsurface Evolution and Persistence of Marine Heatwaves in the Northeast Pacific, Geophys. Res. Lett., 47, e2020GL090548, https://doi.org/10.1029/2020GL090548, 2020.

Schaeffer, A. and Roughan, M.: Subsurface intensification of marine heatwaves off southeastern Australia: The role of stratification and local winds, Geophys. Res. Lett., 44, 5025–5033, https://doi.org/10.1002/2017GL073714, 2017.

Schaeffer, A., Sen Gupta, A., and Roughan, M.: Seasonal stratification and complex local dynamics control the sub-surface structure of marine heatwaves in Eastern Australian coastal waters, Commun. Earth Environ., 4, 304, https://doi.org/10.1038/s43247-023-00966-4, 2023.

Schouten, M. W., De Ruijter, W. P. M., Van Leeuwen, P. J., and Ridderinkhof, H.: Eddies and variability in the Mozambique Channel, Deep Sea Res. Part II Top. Stud. Oceanogr., 50, 1987–2003, https://doi.org/10.1016/S0967-0645(03)00042-0, 2003.

Sen Gupta, A., Thomsen, M., Benthuysen, J. A., Hobday, A. J., Oliver, E., Alexander, L. V., Burrows, M. T., Donat, M. G., Feng, M., Holbrook, N. J., Perkins-Kirkpatrick, S., Moore, P. J., Rodrigues, R. R., Scannell, H. A., Taschetto, A. S., Ummenhofer, C. C., Wernberg, T., and Smale, D. A.: Drivers and impacts of the most extreme marine heatwave events, Sci. Rep., 10, 19359, https://doi.org/10.1038/s41598-020-75445-3, 2020.

Smith, K. E., Sen Gupta, A., Amaya, D., Benthuysen, J. A., Burrows, M. T., Capotondi, A., Filbee–Dexter, K., Frölicher, T. L., Hobday, A. J., Holbrook, N. J., Malan, N., Moore, P. J., Oliver, E. C. J., Richaud, B., Salcedo–Castro, J., Smale, D. A.,

Thomsen, M., and Wernberg, T.: Baseline matters: Challenges and implications of different marine heatwave baselines, Progress in Oceanography, 231, 103404, https://doi.org/10.1016/j.pocean.2024.103404, 2025.

Spillman, C. M., Smith, G. A., Hobday, A. J., and Hartog, J. R.: Onset and Decline Rates of Marine Heatwaves: Global Trends, Seasonal Forecasts and Marine Management, Front. Clim., 3, 801217, https://doi.org/10.3389/fclim.2021.801217, 2021.

Swart, N. C., Lutjeharms, J. R. E., Ridderinkhof, H., and De Ruijter, W. P. M.: Observed characteristics of Mozambique Channel eddies, J. Geophys. Res. Oceans, 115, 2009JC005875, https://doi.org/10.1029/2009JC005875, 2010.

Voldsund, A., Aguiar-González, B., Gammelsrød, T., Krakstad, J.-O., and Ullgren, J.: Observations of the East Madagascar Current system: Dynamics and volume transports, J. Mar. Res., 75, 531–555, https://doi.org/10.1357/002224017821836725, 2017.

Wu, L., Cai, W., Zhang, L., Nakamura, H., Timmermann, A., Joyce, T., McPhaden, M. J., Alexander, M., Qiu, B., Visbeck, M., Chang, P., and Giese, B.: Enhanced warming over the global subtropical western boundary currents, Nat. Clim. Change, 2, 161–166, https://doi.org/10.1038/nclimate1353, 2012.

Wyatt, A. S. J., Leichter, J. J., Washburn, L., Kui, L., Edmunds, P. J., and Burgess, S. C.: Hidden heatwaves and severe coral bleaching linked to mesoscale eddies and thermocline dynamics, Nat. Commun., 14, 25, https://doi.org/10.1038/s41467-022-35550-5, 2023.

Zhang, Y., Du, Y., Feng, M., and Hobday, A. J.: Vertical structures of marine heatwaves, Nat. Commun., 14, 6483, https://doi.org/10.1038/s41467-023-42219-0, 2023.

Zhao, Z., Holbrook, N. J., and Oliver, E. C. J.: An eddy pathway to marine heatwave predictability off eastern Tasmania, Front. Clim., 4, 907828, https://doi.org/10.3389/fclim.2022.907828, 2022.